

# Deep Learning

Lecture 3: Convolutional networks

Prof. Gilles Louppe  
[g.louppe@uliege.be](mailto:g.louppe@uliege.be)



# Today

How to make neural networks see?

- A little history
- Convolutions
- Convolutional network architectures
- Beyond classification
- What is really happening?

# A little history

Adapted from Yannis Avrithis, "Lecture 1: Introduction", [Deep Learning for vision](#), 2018.

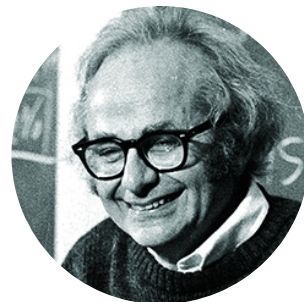
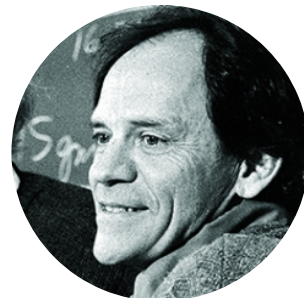
J. Physiol. (1959) 148, 574–591

RECEPTIVE FIELDS OF SINGLE NEURONES IN  
THE CAT'S STRIATE CORTEX

BY D. H. HUBEL\* AND T. N. WIESEL\*

*From the Wilmer Institute, The Johns Hopkins Hospital and  
University, Baltimore, Maryland, U.S.A.*

(Received 22 April 1959)



## Visual perception (Hubel and Wiesel, 1959-1962)

- David Hubel and Torsten Wiesel discover the neural basis of **visual perception**.
- Nobel Prize of Medicine in 1981 for this work.



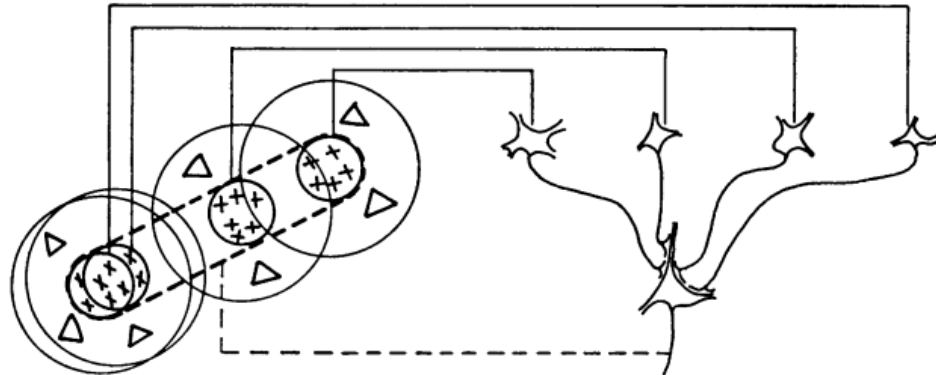
Hubel & Wiesel 1: Intro



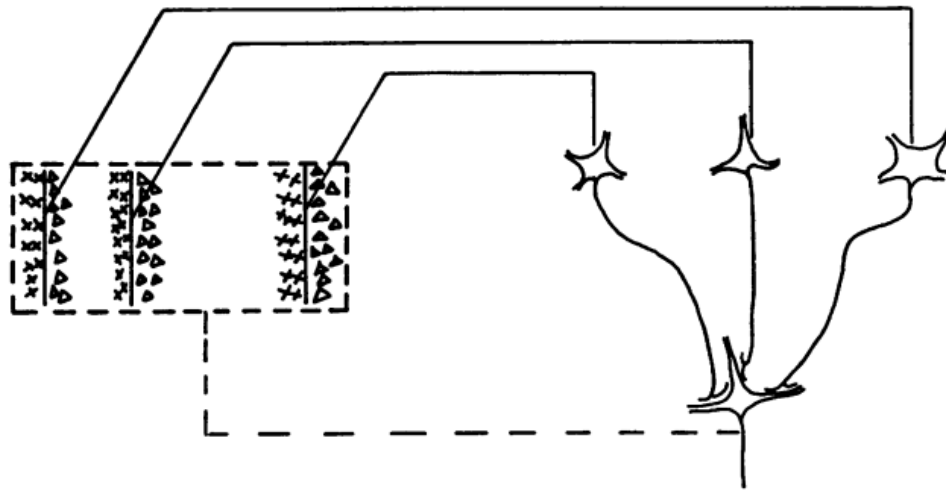
Watch later Share



Hubel and Wiesel

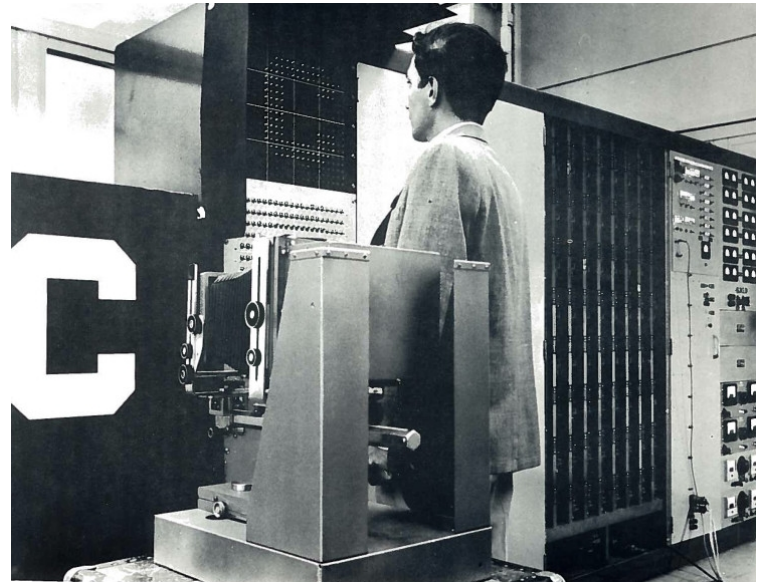
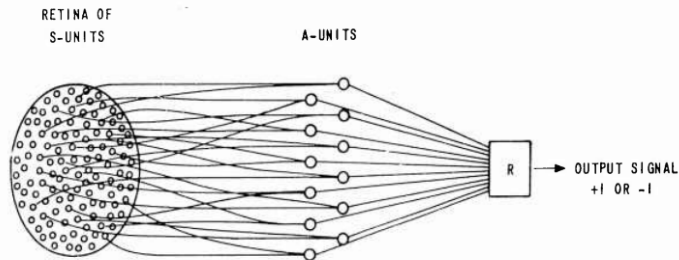


Text-fig. 19. Possible scheme for explaining the organization of simple receptive fields. A large number of lateral geniculate cells, of which four are illustrated in the upper right in the figure, have receptive fields with 'on' centres arranged along a straight line on the retina. All of these project upon a single cortical cell, and the synapses are supposed to be excitatory. The receptive field of the cortical cell will then have an elongated 'on' centre indicated by the interrupted lines in the receptive-field diagram to the left of the figure.



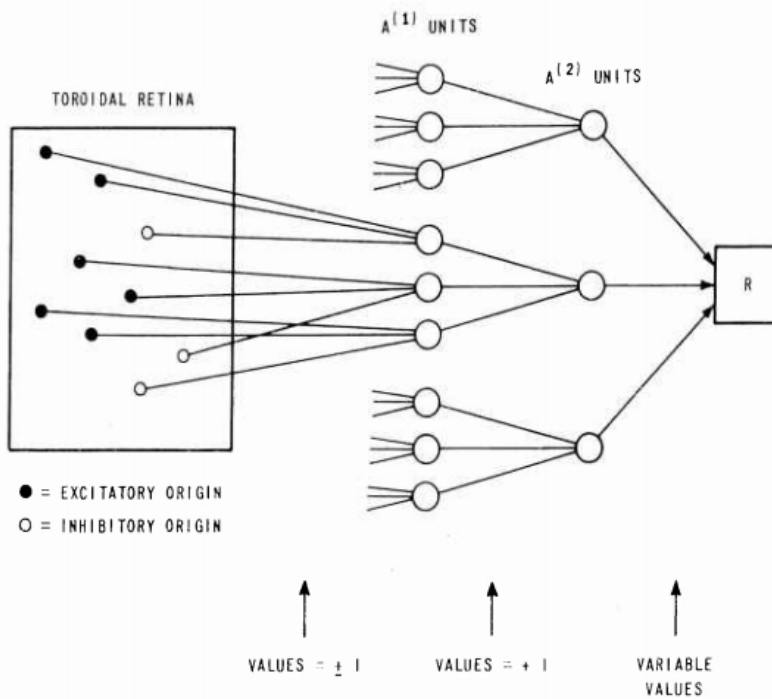
**Text-fig. 20.** Possible scheme for explaining the organization of complex receptive fields. A number of cells with simple fields, of which three are shown schematically, are imagined to project to a single cortical cell of higher order. Each projecting neurone has a receptive field arranged as shown to the left: an excitatory region to the left and an inhibitory region to the right of a vertical straight-line boundary. The boundaries of the fields are staggered within an area outlined by the interrupted lines. Any vertical-edge stimulus falling across this rectangle, regardless of its position, will excite some simple-field cells, leading to excitation of the higher-order cell.

## Perceptron (Rosenblatt, 1959)



The Mark-1 Perceptron:

- Analog circuit implementation of a neural network,
- Parameters as potentiometers.



*"If we show the perceptron a stimulus, say a square, and associate a response to that square, this response will immediately generalize perfectly to all transforms of the square under the transformation group [...]."*

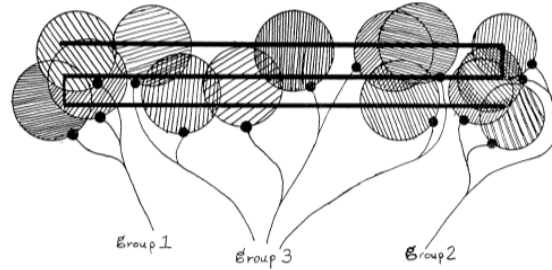
This is quite similar to Hubel and Wiesel's simple and complex cells!

**Theorem 0.8:** No diameter-limited perceptron can determine whether or not all the parts of any geometric figure are connected to one another! That is, no such perceptron computes  $\psi_{\text{CONNECTED}}$ .

The proof requires us to consider just four figures



and a diameter-limited perceptron  $\psi$  whose support sets have diameters like those indicated by the circles below:



## AI winter (Minsky and Papert, 1969+)

- Minsky and Papert redefine the perceptron as a linear classifier,
- Then they prove a series of impossibility results. **AI winter** follows.

Actual Variable	Variable Number (Address)	Category	Major Source	Minor Source
$A(t+1)$	13	sum	12	11
$k_1 A(t)$	12	product	3	1
$k_2^* U(t) \left(\frac{A(t)-U(t)}{A(t)+U(t)}\right)^{k_4}$	11	product	10	4
$U(t) \left(\frac{A(t)-U(t)}{A(t)+U(t)}\right)^{k_4}$	10	product	9	2
$\left(\frac{A(t)-U(t)}{A(t)+U(t)}\right)^{k_4}$	9	power	8	5
$\frac{A(t)-U(t)}{A(t)+U(t)}$	8	ratio	7	6
$A(t)-U(t)$	7	difference	1	2
$A(t)+U(t)$	6	sum	1	2
$k_4$	5	parameter	-	-
$k_2$	4	parameter	-	-
$k_1$	3	parameter	-	-
$U(t)$	2	given	-	-
$A(t)$	1	given	-	-

## Automatic differentiation (Werbos, 1974)

- Formulate an arbitrary function as computational graph.
- Dynamic feedback: compute symbolic derivatives by dynamic programming.

# Neocognitron (Fukushima, 1980)

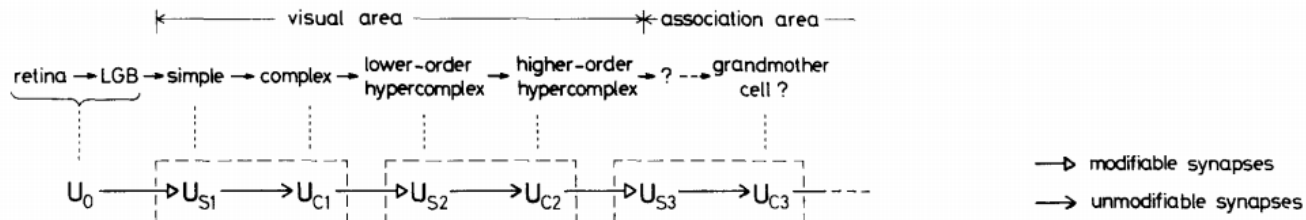


Fig. 1. Correspondence between the hierarchy model by Hubel and Wiesel, and the neural network of the neocognitron

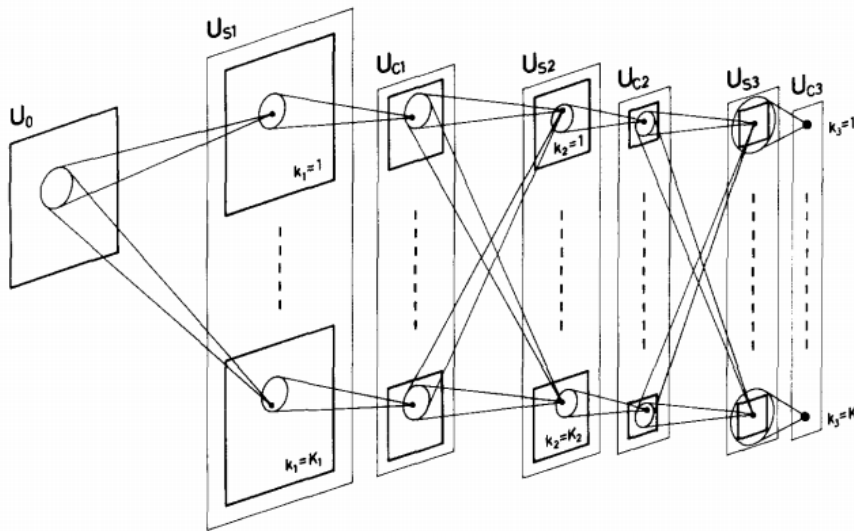
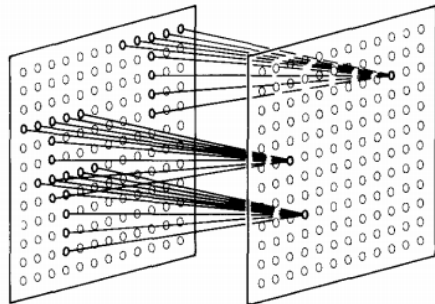
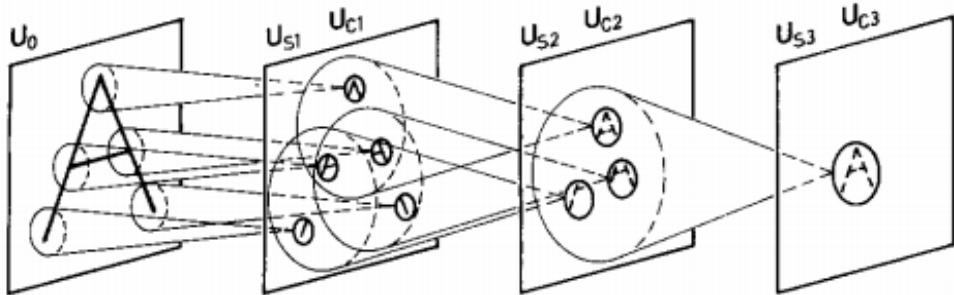


Fig. 2. Schematic diagram illustrating the interconnections between layers in the neocognitron

Fukushima proposes a direct neural network implementation of the hierarchy model of the visual nervous system of Hubel and Wiesel.



Convolutions



Feature hierarchy

- Built upon **convolutions** and enables the composition of a **feature hierarchy**.
- Biologically-inspired training algorithm, which proves to be largely inefficient.

## Backpropagation (Rumelhart et al, 1986)

- Introduce backpropagation in multi-layer networks with sigmoid non-linearities and sum of squares loss function.
- Advocate batch gradient descent for supervised learning.
- Discuss online gradient descent, momentum and random initialization.
- Depart from biologically plausible training algorithms.

The backward pass starts by computing  $\partial E / \partial y$  for each of the output units. Differentiating equation (3) for a particular case,  $c$ , and suppressing the index  $c$  gives

$$\partial E / \partial y_j = y_j - d_j \quad (4)$$

We can then apply the chain rule to compute  $\partial E / \partial x_j$ ,

$$\partial E / \partial x_j = \partial E / \partial y_j \cdot dy_j / dx_j$$

Differentiating equation (2) to get the value of  $dy_j / dx_j$  and substituting gives

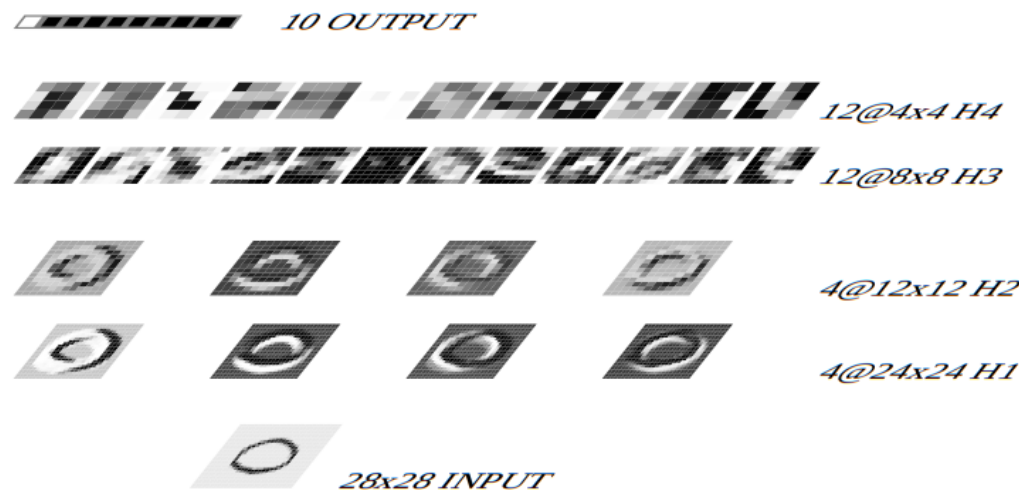
$$\partial E / \partial x_j = \partial E / \partial y_j \cdot y_j(1 - y_j) \quad (5)$$

This means that we know how a change in the total input  $x$  to an output unit will affect the error. But this total input is just a linear function of the states of the lower level units and it is also a linear function of the weights on the connections, so it is easy to compute how the error will be affected by changing these states and weights. For a weight  $w_{ji}$ , from  $i$  to  $j$  the derivative is

$$\begin{aligned} \partial E / \partial w_{ji} &= \partial E / \partial x_j \cdot \partial x_j / \partial w_{ji} \\ &= \partial E / \partial x_j \cdot y_i \end{aligned} \quad (6)$$

## Convolutional networks (LeCun, 1990)

- Train a convolutional network by backpropagation.
- Advocate end-to-end feature learning for image classification.





Convolutional Network Demo from 1993



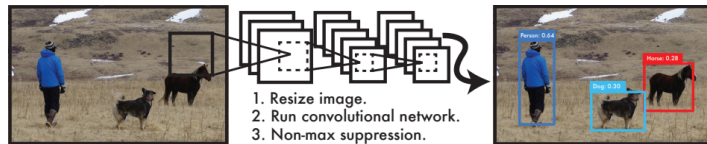
Watch later

Share

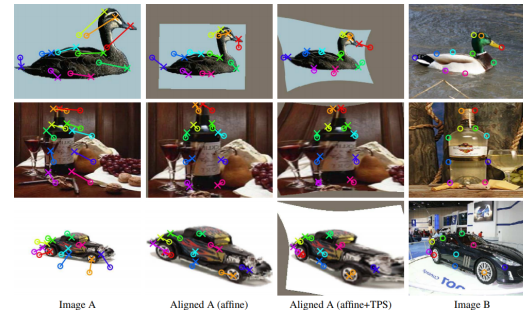


LeNet-1 (LeCun et al, 1993)

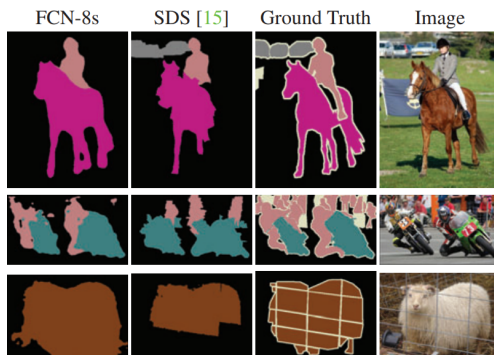
Convolutional networks are now **used everywhere in vision.**



Object detection  
(Redmon et al, 2015)



Geometric matching  
(Rocco et al, 2017)



Semantic segmentation  
(Long et al, 2015)

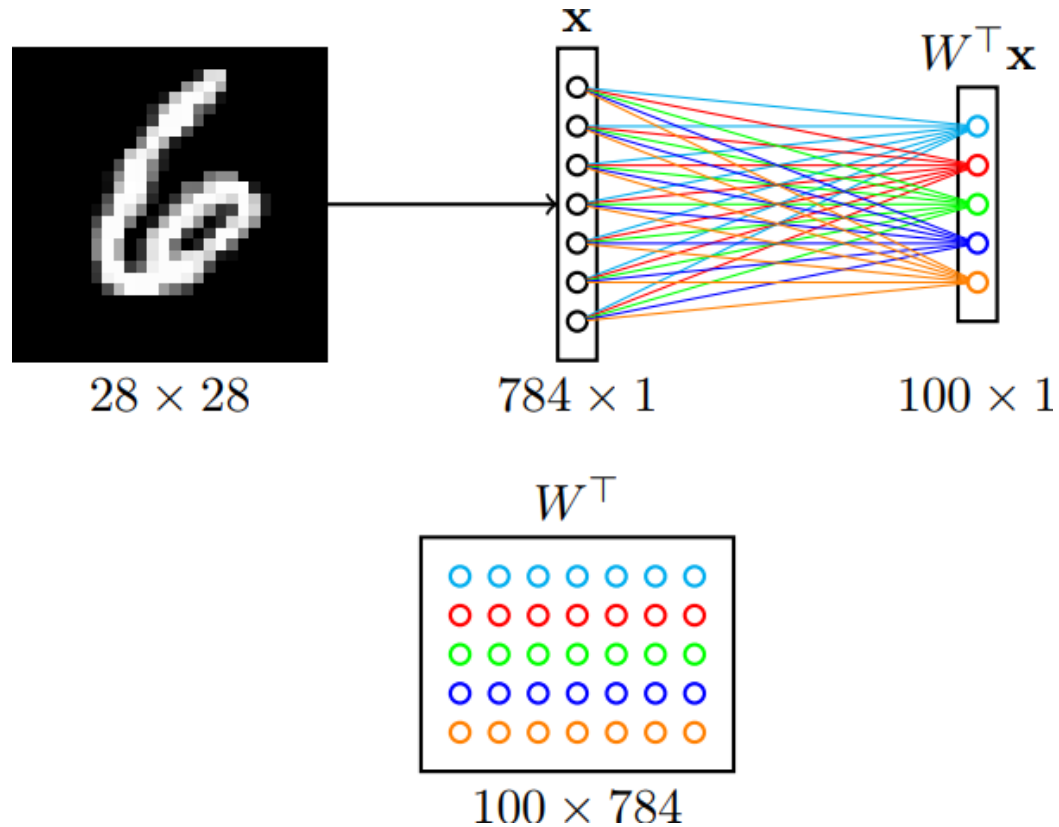


Instance segmentation  
(He et al, 2017)

... but also in many other applications, including:

- speech recognition and synthesis
- natural language processing
- protein/DNA binding prediction
- or more generally, any problem **with a spatial** (or sequential) **structure**.

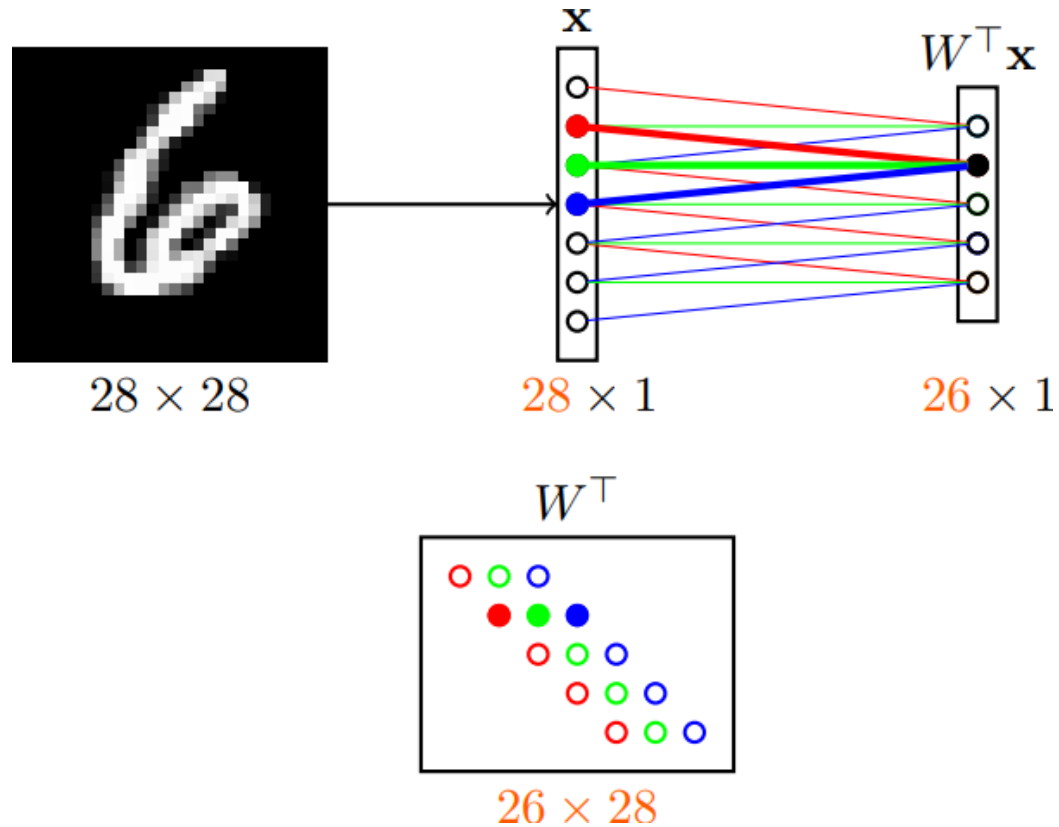
# Convolutions



Let us consider the first layer of a MLP taking images as input. What are the problems with this architecture?

## Issues

- Too many parameters:  $100 \times 784 + 100$ .
  - What if images are  $640 \times 480 \times 3$ ?
  - What if the first layer counts  $1000$  units?
- Spatial organization of the input is destroyed.
- The network is not invariant to transformations (e.g., translation).



Instead, let us only keep a **sparse** set of connections, where all weights having the same color are **shared**.

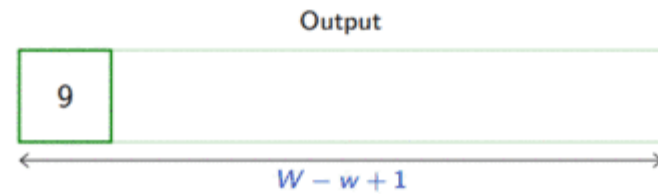
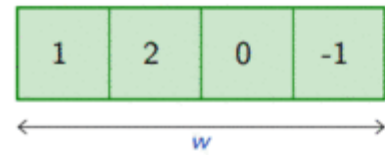
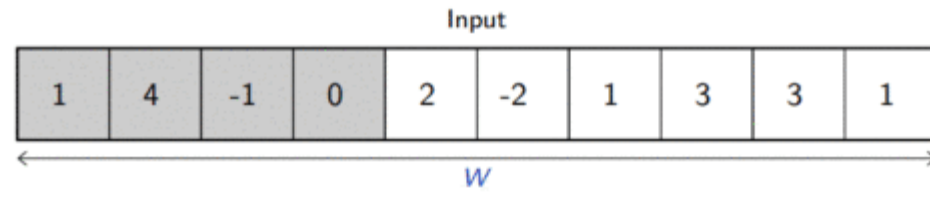
- The resulting operation can be seen as **shifting** the same weight triplet (**kernel**).
  - The set of inputs seen by each unit is its **receptive field**.
- ⇒ This is a 1D **convolution**, which can be generalized to more dimensions.

# Convolutions

For one-dimensional tensors, given an input vector  $\mathbf{x} \in \mathbb{R}^W$  and a convolutional kernel  $\mathbf{u} \in \mathbb{R}^w$ , the discrete **convolution**  $\mathbf{u} \star \mathbf{x}$  is a vector of size  $W - w + 1$  such that

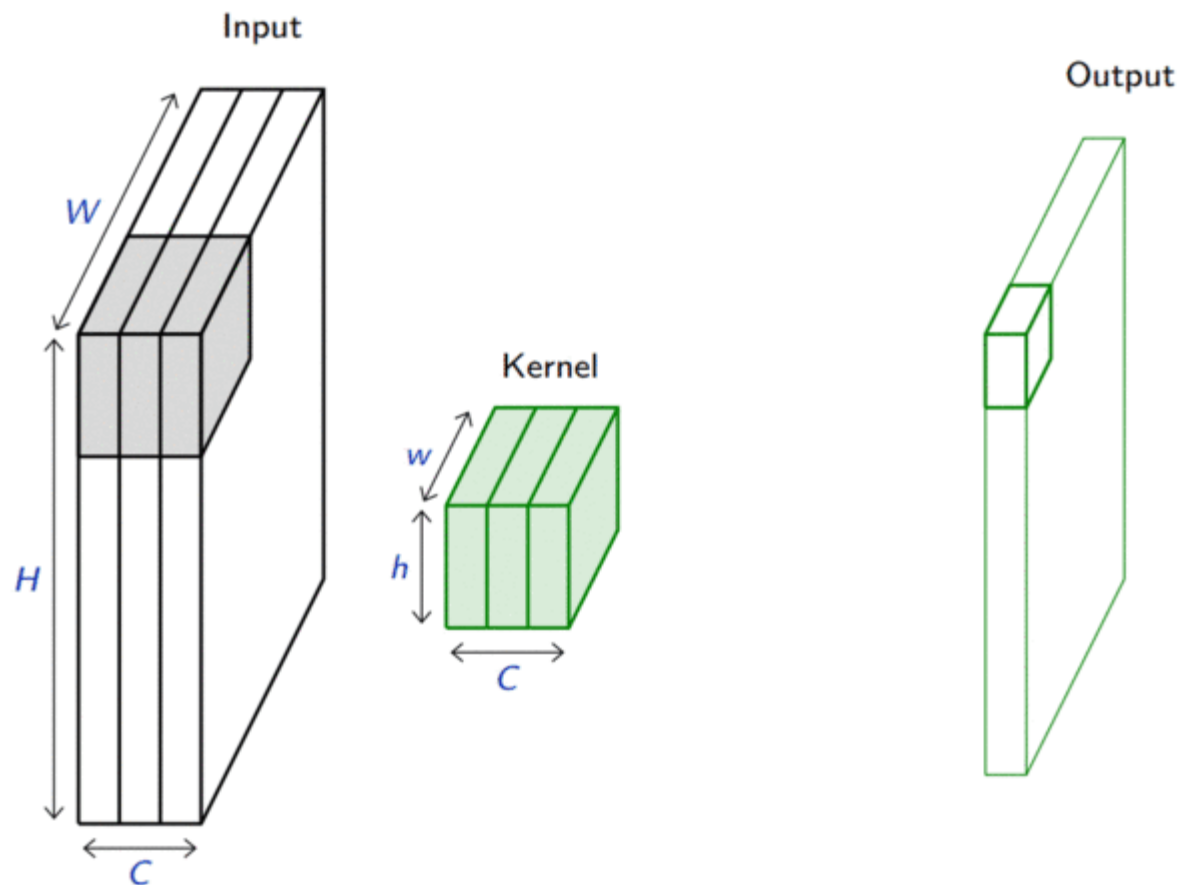
$$(\mathbf{u} \star \mathbf{x})[i] = \sum_{m=0}^{w-1} u_m x_{m+i}.$$

- Technically,  $\star$  denotes the **cross-correlation** operator.
- However, most machine learning libraries call it convolution.



Convolutions generalize to multi-dimensional tensors:

- In its most usual form, a convolution takes as input a 3D tensor  $\mathbf{x} \in \mathbb{R}^{C \times H \times W}$ , called the **input feature map**.
- A kernel  $\mathbf{u} \in \mathbb{R}^{C \times h \times w}$  slides across the input feature map, along its height and width. The size  $h \times w$  is the size of the receptive field.
- At each location, the element-wise product between the kernel and the input elements it overlaps is computed and the results are summed up.



- The final output  $\mathbf{o}$  is a 2D tensor of size  $(H - h + 1) \times (W - w + 1)$  called the **output feature map** and such that:

$$\mathbf{o}_{j,i} = \mathbf{b}_{j,i} + \sum_{c=0}^{C-1} (\mathbf{u}_c \star \mathbf{x}_c)[j, i] = \mathbf{b}_{j,i} + \sum_{c=0}^{C-1} \sum_{n=0}^{h-1} \sum_{m=0}^{w-1} \mathbf{u}_{c,n,m} \mathbf{x}_{c,n+j,m+i}$$

where  $\mathbf{u}$  and  $\mathbf{b}$  are shared parameters to learn.

- $D$  convolutions can be applied in the same way to produce a  $D \times (H - h + 1) \times (W - w + 1)$  feature map, where  $D$  is the depth.

## Convolution as a matrix multiplication

As a guiding example, let us consider the convolution of single-channel tensors  $\mathbf{x} \in \mathbb{R}^{4 \times 4}$  and  $\mathbf{u} \in \mathbb{R}^{3 \times 3}$ :

$$\mathbf{u} \star \mathbf{x} = \begin{pmatrix} 1 & 4 & 1 \\ 1 & 4 & 3 \\ 3 & 3 & 1 \end{pmatrix} \star \begin{pmatrix} 4 & 5 & 8 & 7 \\ 1 & 8 & 8 & 8 \\ 3 & 6 & 6 & 4 \\ 6 & 5 & 7 & 8 \end{pmatrix} = \begin{pmatrix} 122 & 148 \\ 126 & 134 \end{pmatrix}$$

The convolution operation can be equivalently re-expressed as a single matrix multiplication:

- the convolutional kernel  $\mathbf{u}$  is rearranged as a **sparse Toeplitz circulant matrix**, called the convolution matrix:

$$\mathbf{U} = \begin{pmatrix} 1 & 4 & 1 & 0 & 1 & 4 & 3 & 0 & 3 & 3 & 1 & 0 & 0 & 0 & 0 & 0 \\ 0 & 1 & 4 & 1 & 0 & 1 & 4 & 3 & 0 & 3 & 3 & 1 & 0 & 0 & 0 & 0 \\ 0 & 0 & 0 & 0 & 1 & 4 & 1 & 0 & 1 & 4 & 3 & 0 & 3 & 3 & 1 & 0 \\ 0 & 0 & 0 & 0 & 0 & 1 & 4 & 1 & 0 & 1 & 4 & 3 & 0 & 3 & 3 & 1 \end{pmatrix}$$

- the input  $\mathbf{x}$  is flattened row by row, from top to bottom:

$$v(\mathbf{x}) = (4 \quad 5 \quad 8 \quad 7 \quad 1 \quad 8 \quad 8 \quad 8 \quad 3 \quad 6 \quad 6 \quad 4 \quad 6 \quad 5 \quad 7 \quad 8)^T$$

Then,

$$\mathbf{U}v(\mathbf{x}) = (122 \quad 148 \quad 126 \quad 134)^T$$

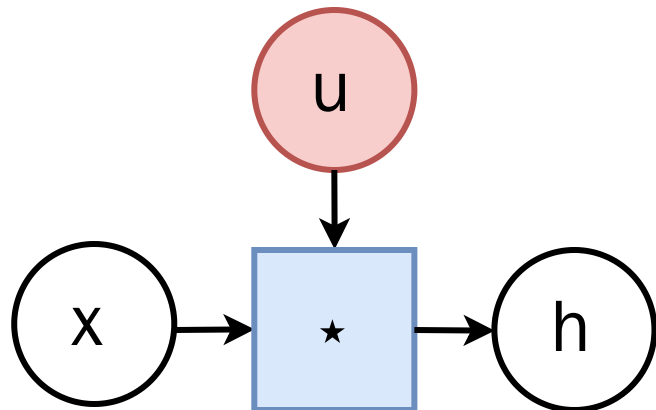
which we can reshape to a  $2 \times 2$  matrix to obtain  $\mathbf{u} \star \mathbf{x}$ .

The same procedure generalizes to  $\mathbf{x} \in \mathbb{R}^{H \times W}$  and convolutional kernel  $\mathbf{u} \in \mathbb{R}^{h \times w}$ , such that:

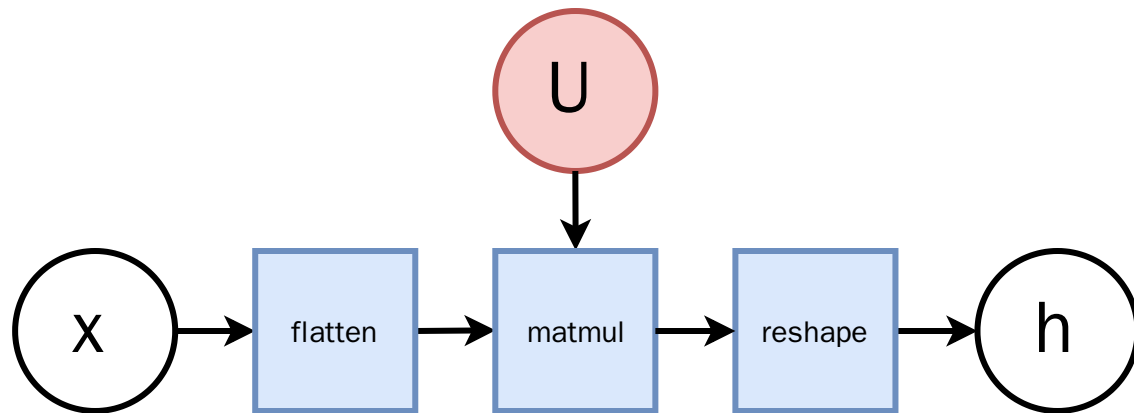
- the convolutional kernel is rearranged as a sparse Toeplitz circulant matrix  $\mathbf{U}$  of shape  $(H - h + 1)(W - w + 1) \times HW$  where
  - each row  $i$  identifies an element of the output feature map,
  - each column  $j$  identifies an element of the input feature map,
  - the value  $\mathbf{U}_{i,j}$  corresponds to the kernel value the element  $j$  is multiplied with in output  $i$ ;
- the input  $\mathbf{x}$  is flattened into a column vector  $v(\mathbf{x})$  of shape  $HW \times 1$ ;
- the output feature map  $\mathbf{u} \star \mathbf{x}$  is obtained by reshaping the  $(H - h + 1)(W - w + 1) \times 1$  column vector  $\mathbf{U}v(\mathbf{x})$  as a  $(H - h + 1) \times (W - w + 1)$  matrix.

Therefore, a convolutional layer is a special case of a fully connected layer:

$$\mathbf{h} = \mathbf{u} \star \mathbf{x} \Leftrightarrow v(\mathbf{h}) = \mathbf{U}v(\mathbf{x}) \Leftrightarrow v(\mathbf{h}) = \mathbf{W}^T v(\mathbf{x})$$

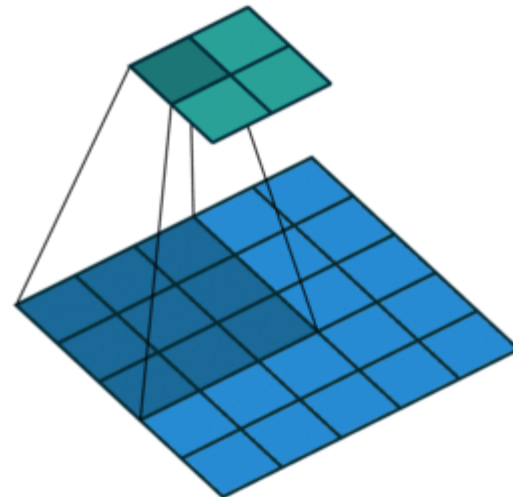


$\Leftrightarrow$



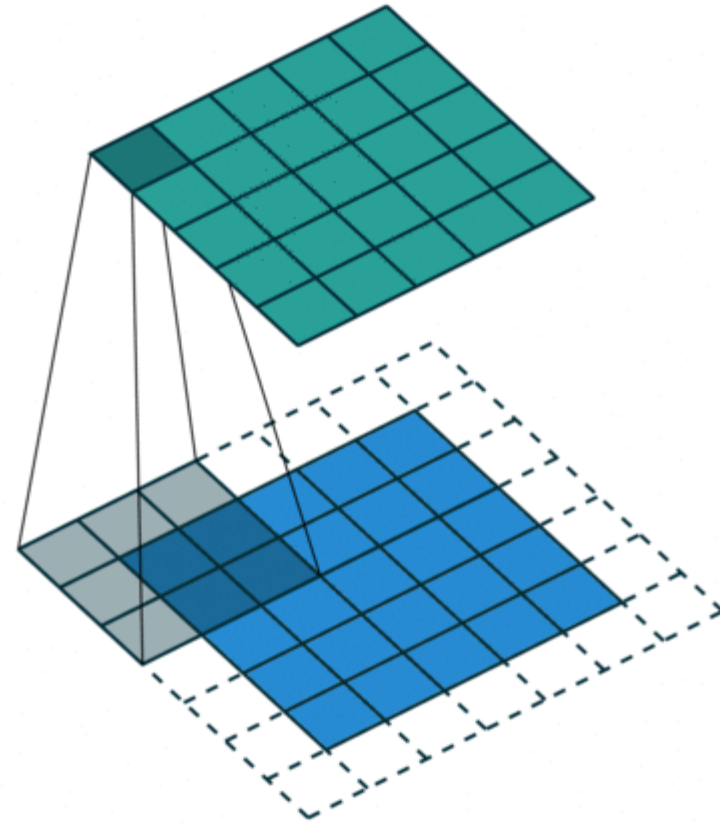
## Strides

- The **stride** specifies the size of the step for the convolution operator.
- This parameter reduces the size of the output map.



## Padding

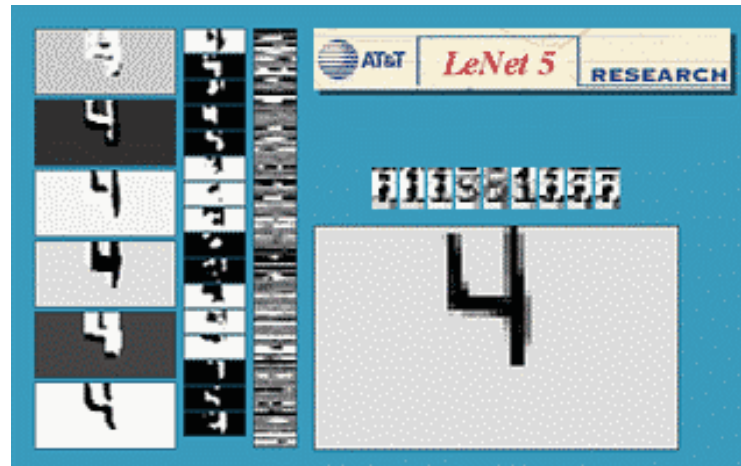
- Padding specifies whether the input volume is padded artificially around its border.
- This parameter is useful to keep spatial dimensions constant across filters.
- Zero-padding is the default mode.



# Equivariance

A function  $f$  is **equivariant** to  $g$  if  $f(g(\mathbf{x})) = g(f(\mathbf{x}))$ .

- Parameter sharing used in a convolutional layer causes the layer to be equivariant to translation.
- That is, if  $g$  is any function that translates the input, the convolution function is equivariant to  $g$ .



*If an object moves in the input image, its representation will move the same amount in the output.*

- Equivariance is useful when we know some local function is useful everywhere (e.g., edge detectors).
- Convolution is not equivariant to other operations such as change in scale or rotation.

# Pooling

When the input volume is large, **pooling layers** can be used to reduce the input dimension while preserving its global structure, in a way similar to a down-scaling operation.

Consider a pooling area of size  $h \times w$  and a 3D input tensor  $\mathbf{x} \in \mathbb{R}^{C \times (rh) \times (sw)}$ .

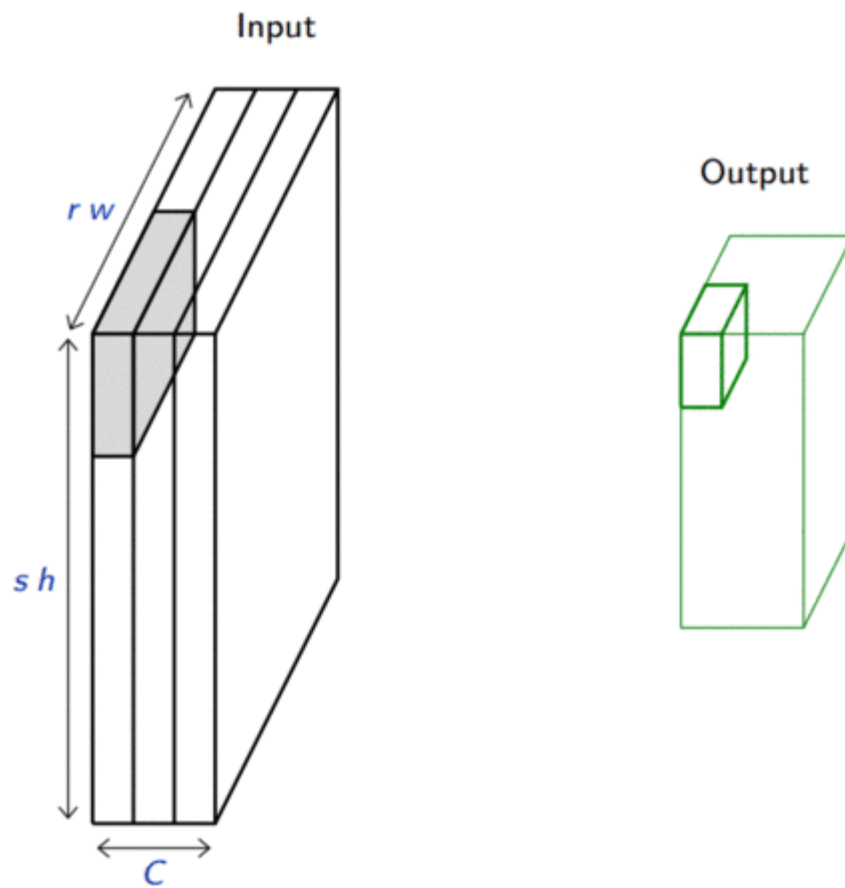
- Max-pooling produces a tensor  $\mathbf{o} \in \mathbb{R}^{C \times r \times s}$  such that

$$\mathbf{o}_{c,j,i} = \max_{n < h, m < w} \mathbf{x}_{c,rj+n,si+m}.$$

- Average pooling produces a tensor  $\mathbf{o} \in \mathbb{R}^{C \times r \times s}$  such that

$$\mathbf{o}_{c,j,i} = \frac{1}{hw} \sum_{n=0}^{h-1} \sum_{m=0}^{w-1} \mathbf{x}_{c,rj+n,si+m}.$$

Pooling is very similar in its formulation to convolution.



## Invariance

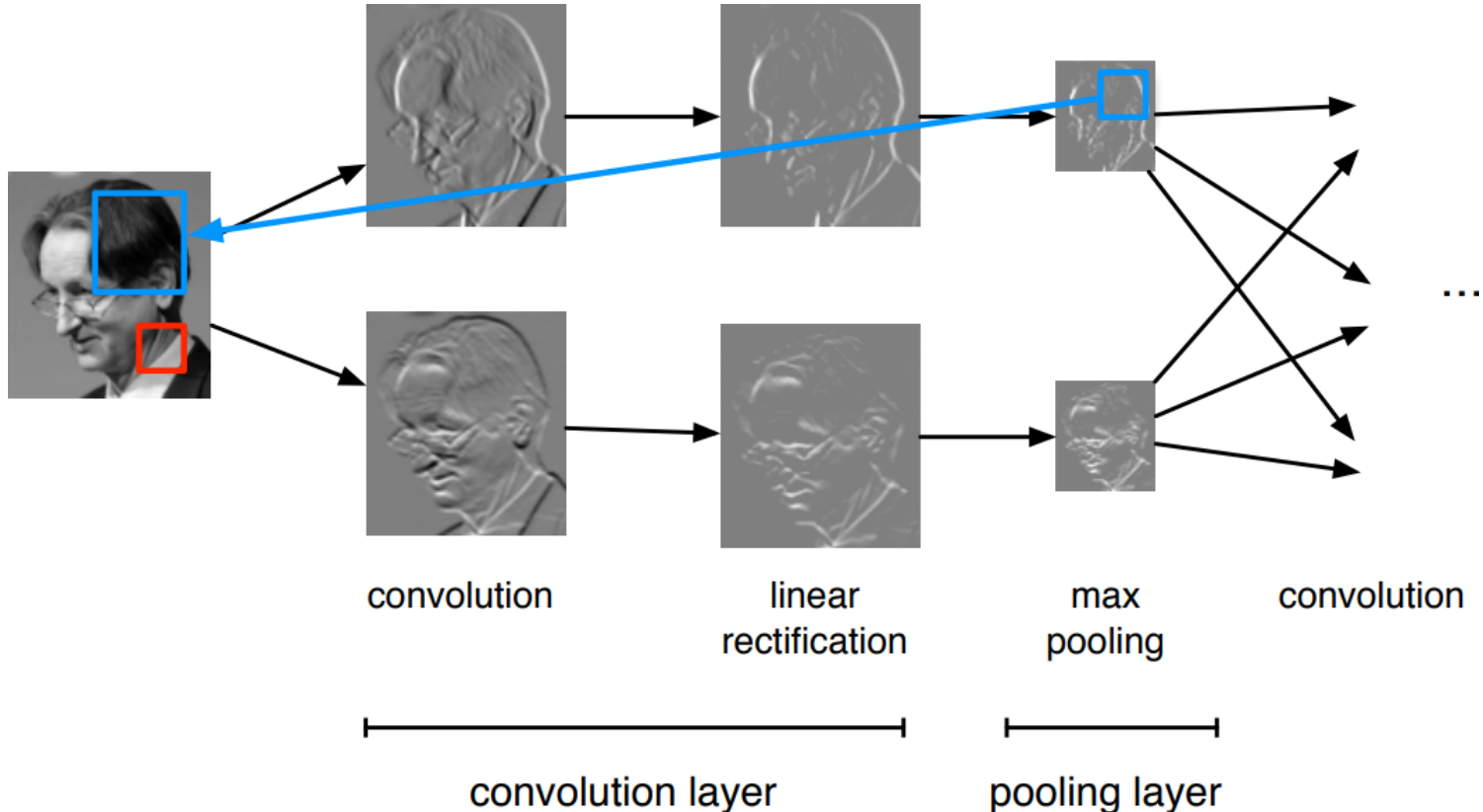
A function  $f$  is **invariant** to  $g$  if  $f(g(\mathbf{x})) = f(\mathbf{x})$ .

- Pooling layers can be used for building inner activations that are (slightly) invariant to small translations of the input.
- Invariance to local translation is helpful if we care more about the presence of a pattern rather than its exact position.

# Architectures

# Layer patterns

A **convolutional network** can often be defined as a composition of convolutional layers (**CONV**), pooling layers (**POOL**), linear rectifiers (**RELU**) and fully connected layers (**FC**).



The most common convolutional network architecture follows the pattern:

**INPUT** → [[**CONV** → **RELU**]\* $N$  → **POOL?**]\* $M$  → [**FC** → **RELU**]\* $K$  → **FC**

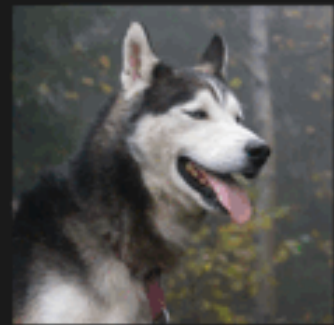
where:

- \* indicates repetition;
- **POOL?** indicates an optional pooling layer;
- $N \geq 0$  (and usually  $N \leq 3$ ),  $M \geq 0$ ,  $K \geq 0$  (and usually  $K < 3$ );
- the last fully connected layer holds the output (e.g., the class scores).

# Architectures

Some common architectures for convolutional networks following this pattern include:

- INPUT → FC, which implements a linear classifier ( $N = M = K = 0$ ).
- INPUT → [FC → RELU] $*K$  → FC, which implements a  $K$ -layer MLP.
- INPUT → CONV → RELU → FC.
- INPUT → [CONV → RELU → POOL] $*2$  → FC → RELU → FC.
- INPUT → [[CONV → RELU] $*2$  → POOL] $*3$  → [FC → RELU] $*2$  → FC.



## LeNet-5 (LeCun et al, 1998)

- First convolutional network to use backpropagation.
- Applied to character recognition.

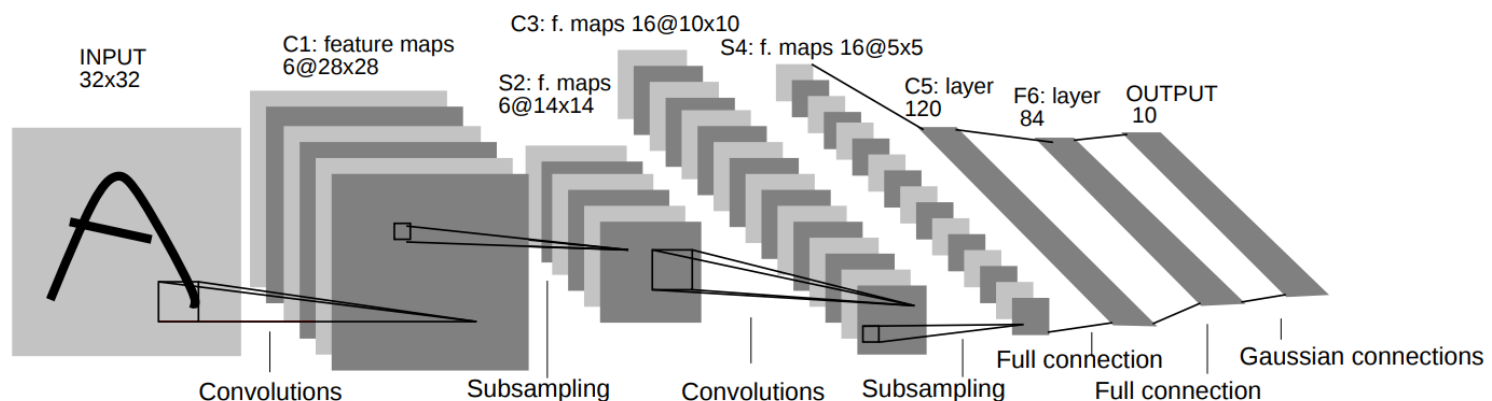


Fig. 2. Architecture of LeNet-5, a Convolutional Neural Network, here for digits recognition. Each plane is a feature map, i.e. a set of units whose weights are constrained to be identical.

Layer (type)	Output Shape	Param #
<hr/>		
Conv2d-1	[ -1, 6, 28, 28]	156
ReLU-2	[ -1, 6, 28, 28]	0
MaxPool2d-3	[ -1, 6, 14, 14]	0
Conv2d-4	[ -1, 16, 10, 10]	2,416
ReLU-5	[ -1, 16, 10, 10]	0
MaxPool2d-6	[ -1, 16, 5, 5]	0
Conv2d-7	[ -1, 120, 1, 1]	48,120
ReLU-8	[ -1, 120, 1, 1]	0
Linear-9	[ -1, 84]	10,164
ReLU-10	[ -1, 84]	0
Linear-11	[ -1, 10]	850
LogSoftmax-12	[ -1, 10]	0
<hr/>		
Total params: 61,706		
Trainable params: 61,706		
Non-trainable params: 0		
<hr/>		
Input size (MB): 0.00		
Forward/backward pass size (MB): 0.11		
Params size (MB): 0.24		
Estimated Total Size (MB): 0.35		
<hr/>		

## AlexNet (Krizhevsky et al, 2012)

- 16.4% top-5 error on ILSVRC'12, outperformed all by 10%.
- Implementation on two GPUs, because of memory constraints.

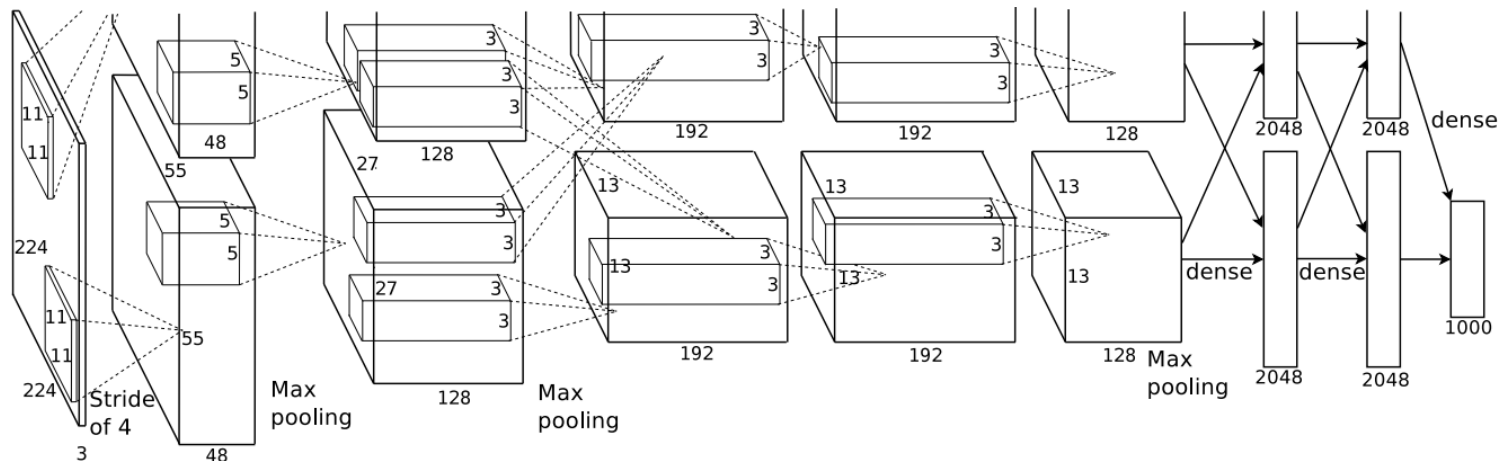


Figure 2: An illustration of the architecture of our CNN, explicitly showing the delineation of responsibilities between the two GPUs. One GPU runs the layer-parts at the top of the figure while the other runs the layer-parts at the bottom. The GPUs communicate only at certain layers. The network's input is 150,528-dimensional, and the number of neurons in the network's remaining layers is given by 253,440–186,624–64,896–64,896–43,264–4096–4096–1000.

Layer (type)	Output Shape	Param #
Conv2d-1	[ -1, 64, 55, 55]	23,296
ReLU-2	[ -1, 64, 55, 55]	0
MaxPool2d-3	[ -1, 64, 27, 27]	0
Conv2d-4	[ -1, 192, 27, 27]	307,392
ReLU-5	[ -1, 192, 27, 27]	0
MaxPool2d-6	[ -1, 192, 13, 13]	0
Conv2d-7	[ -1, 384, 13, 13]	663,936
ReLU-8	[ -1, 384, 13, 13]	0
Conv2d-9	[ -1, 256, 13, 13]	884,992
ReLU-10	[ -1, 256, 13, 13]	0
Conv2d-11	[ -1, 256, 13, 13]	590,080
ReLU-12	[ -1, 256, 13, 13]	0
MaxPool2d-13	[ -1, 256, 6, 6]	0
Dropout-14	[ -1, 9216]	0
Linear-15	[ -1, 4096]	37,752,832
ReLU-16	[ -1, 4096]	0
Dropout-17	[ -1, 4096]	0
Linear-18	[ -1, 4096]	16,781,312
ReLU-19	[ -1, 4096]	0
Linear-20	[ -1, 1000]	4,097,000

Total params: 61,100,840

Trainable params: 61,100,840

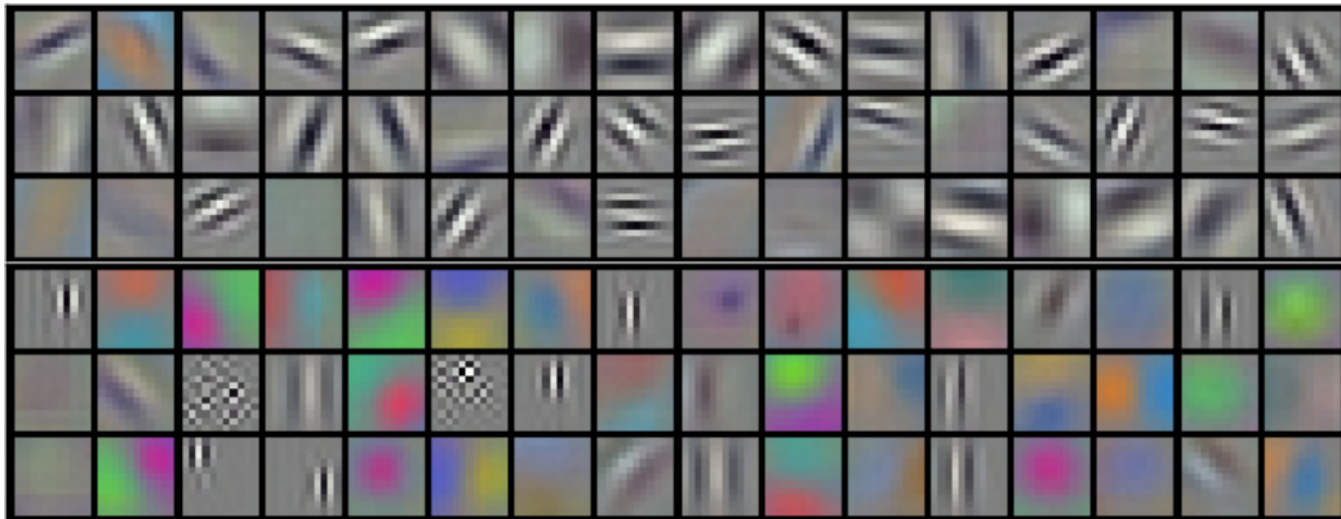
Non-trainable params: 0

Input size (MB): 0.57

Forward/backward pass size (MB): 8.31

Params size (MB): 233.08

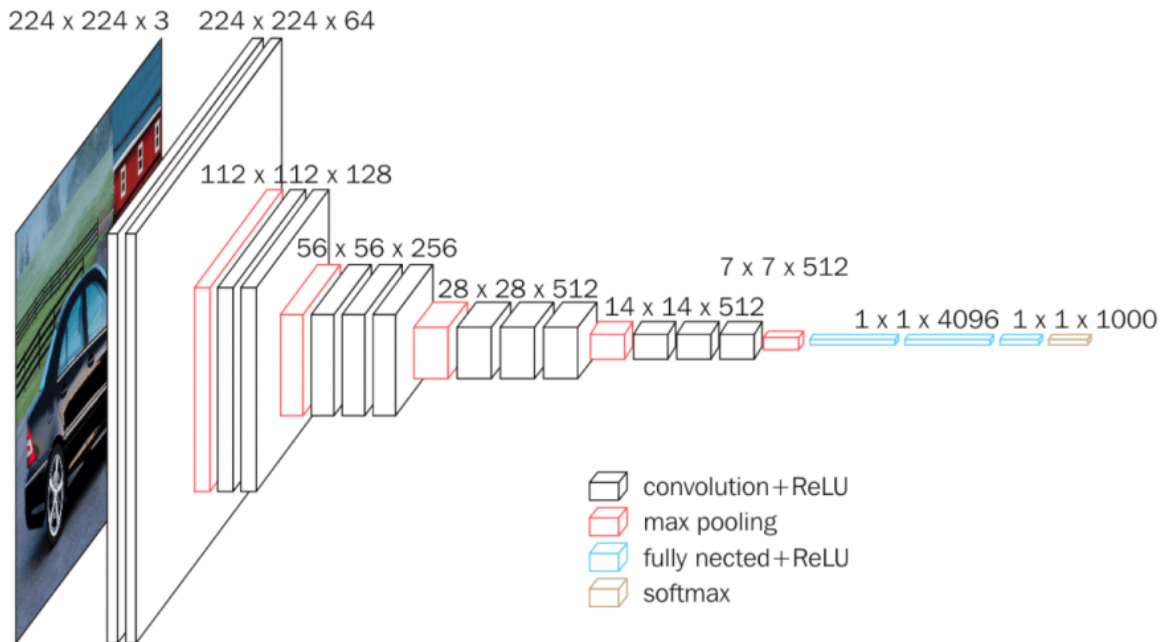
Estimated Total Size (MB): 241.96



- 96  $11 \times 11 \times 3$  kernels learned by the first convolutional layer.
- Top 48 kernels were learned on GPU1, while the bottom 48 kernels were learned on GPU 2.

## VGG (Simonyan and Zisserman, 2014)

- 7.3% top-5 error on ILSVRC'14.
- Depth increased up to 19 layers, kernel sizes reduced to 3.



Layer (type)	Output Shape	Param #
Conv2d-1	[ -1, 64, 224, 224]	1,792
ReLU-2	[ -1, 64, 224, 224]	0
Conv2d-3	[ -1, 64, 224, 224]	36,928
ReLU-4	[ -1, 64, 224, 224]	0
MaxPool2d-5	[ -1, 64, 112, 112]	0
Conv2d-6	[ -1, 128, 112, 112]	73,856
ReLU-7	[ -1, 128, 112, 112]	0
Conv2d-8	[ -1, 128, 112, 112]	147,584
ReLU-9	[ -1, 128, 112, 112]	0
MaxPool2d-10	[ -1, 128, 56, 56]	0
Conv2d-11	[ -1, 256, 56, 56]	295,168
ReLU-12	[ -1, 256, 56, 56]	0
Conv2d-13	[ -1, 256, 56, 56]	590,080
ReLU-14	[ -1, 256, 56, 56]	0
Conv2d-15	[ -1, 256, 56, 56]	590,080
ReLU-16	[ -1, 256, 56, 56]	0
MaxPool2d-17	[ -1, 256, 28, 28]	0
Conv2d-18	[ -1, 512, 28, 28]	1,180,160
ReLU-19	[ -1, 512, 28, 28]	0
Conv2d-20	[ -1, 512, 28, 28]	2,359,808
ReLU-21	[ -1, 512, 28, 28]	0
Conv2d-22	[ -1, 512, 28, 28]	2,359,808
ReLU-23	[ -1, 512, 28, 28]	0
MaxPool2d-24	[ -1, 512, 14, 14]	0
Conv2d-25	[ -1, 512, 14, 14]	2,359,808
ReLU-26	[ -1, 512, 14, 14]	0
Conv2d-27	[ -1, 512, 14, 14]	2,359,808
ReLU-28	[ -1, 512, 14, 14]	0
Conv2d-29	[ -1, 512, 14, 14]	2,359,808
ReLU-30	[ -1, 512, 14, 14]	0
MaxPool2d-31	[ -1, 512, 7, 7]	0
Linear-32	[ -1, 4096]	102,764,544
ReLU-33	[ -1, 4096]	0
Dropout-34	[ -1, 4096]	0
Linear-35	[ -1, 4096]	16,781,312
ReLU-36	[ -1, 4096]	0
Dropout-37	[ -1, 4096]	0
Linear-38	[ -1, 1000]	4,097,000

Total params: 138,357,544

Trainable params: 138,357,544

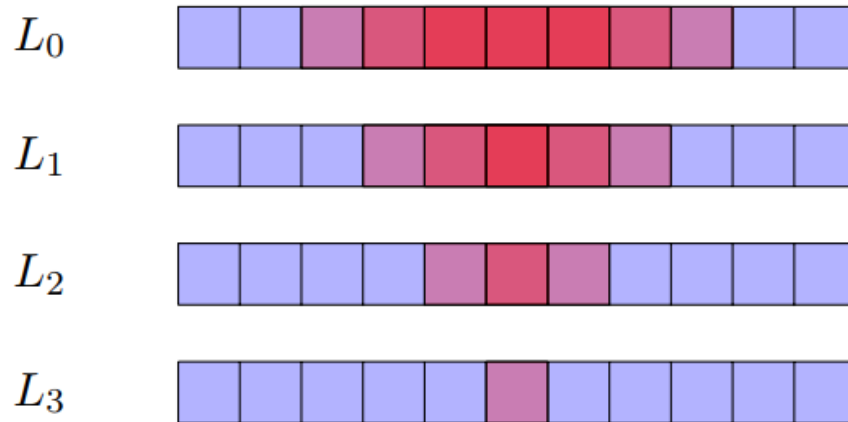
Non-trainable params: 0

Input size (MB): 0.57

Forward/backward pass size (MB): 218.59

Params size (MB): 527.79

Estimated Total Size (MB): 746.96



The **effective receptive field** is the part of the visual input that affects a given unit indirectly through previous layers.

- It grows linearly with depth.
- A stack of three  $3 \times 3$  kernels of stride 1 has the same effective receptive field as a single  $7 \times 7$  kernel, but fewer parameters.

# ResNet (He et al, 2015)

- Even deeper models (34, 50, 101 and 152 layers)
- Skip connections.
- Resnet-50 vs. VGG:
  - 5.25% top-5 error vs. 7.1%
  - 25M vs. 138M parameters
  - 3.8B Flops vs. 15.3B Flops
  - Fully convolutional until the last layer

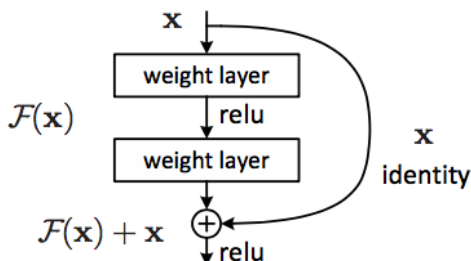
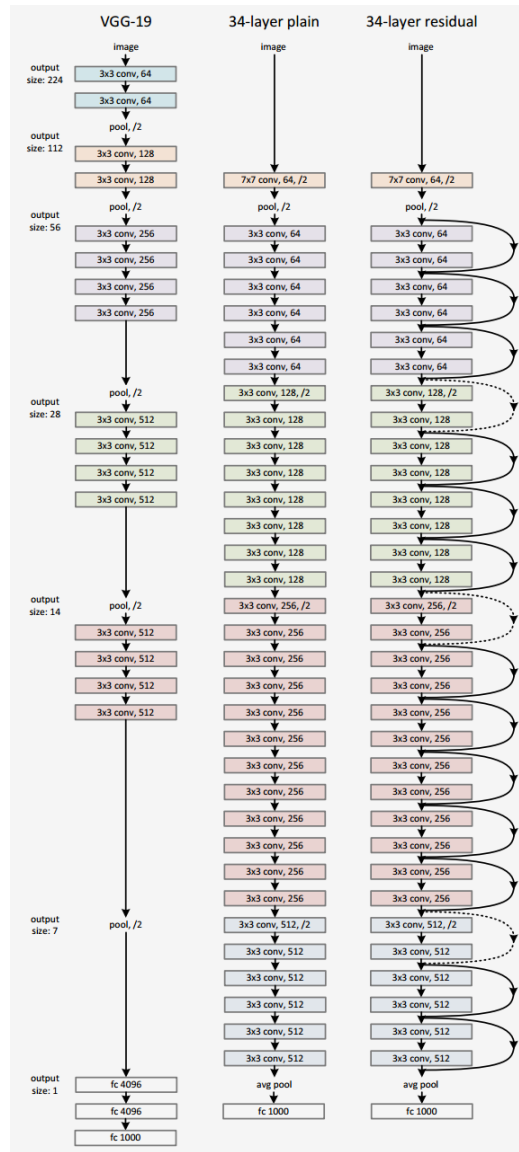
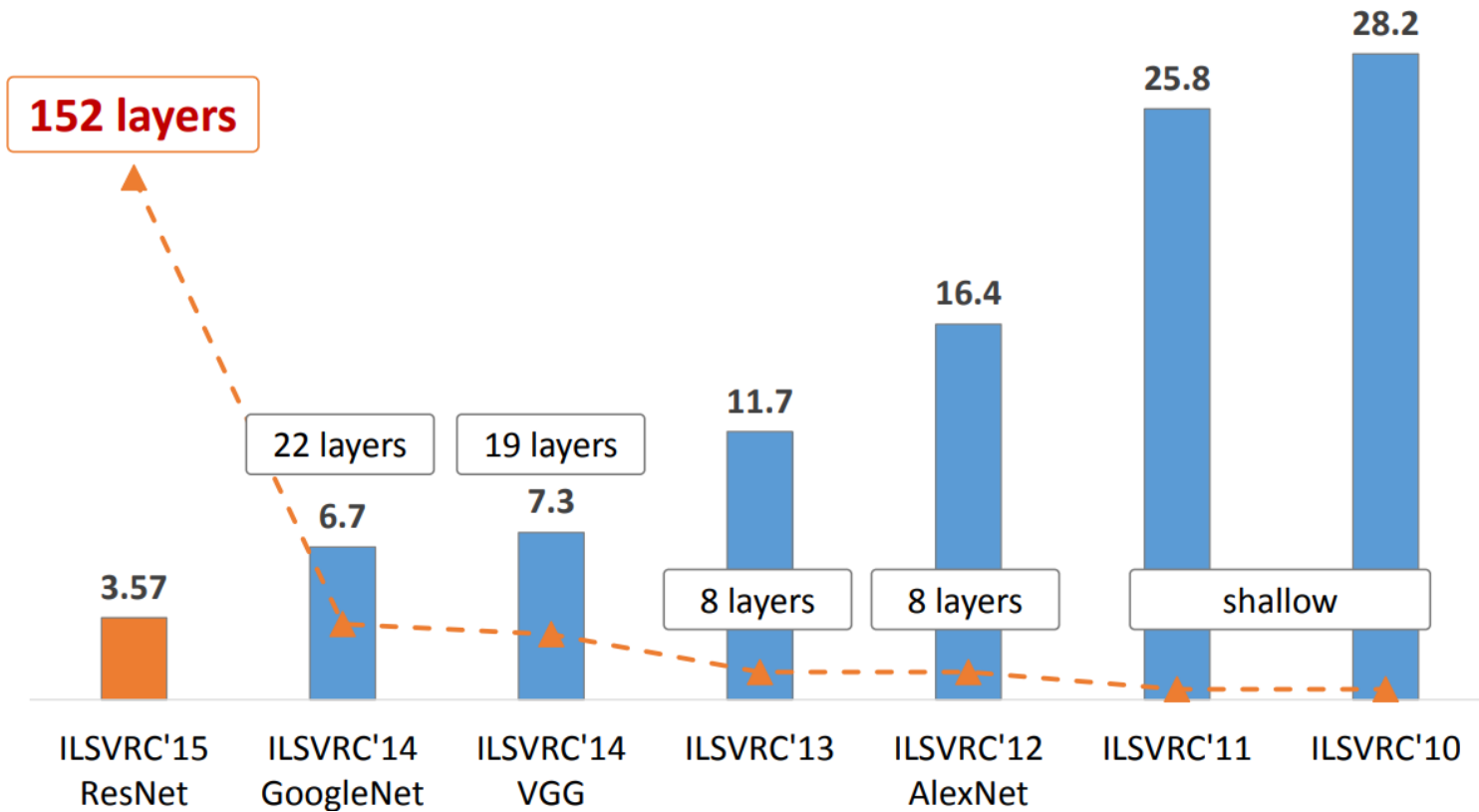


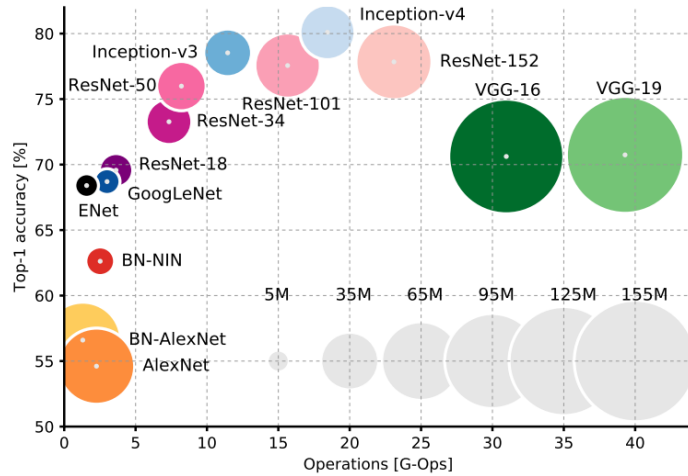
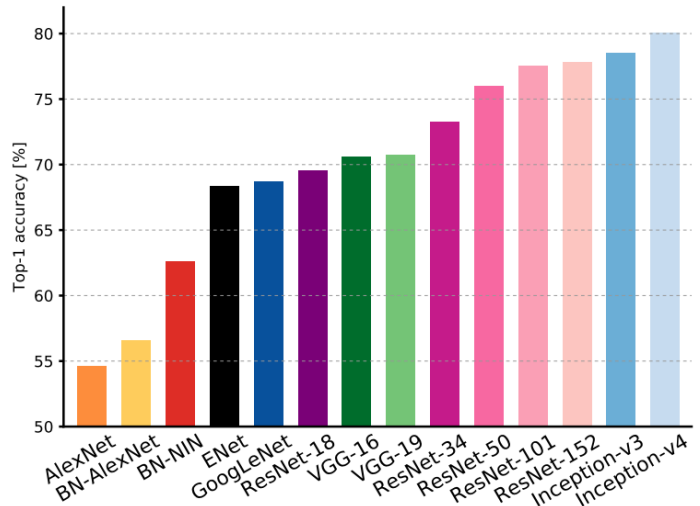
Figure 2. Residual learning: a building block.



Layer (type)	Output Shape	Param #	...
Conv2d-1	[−1, 64, 112, 112]	9,408	Bottleneck-130
BatchNorm2d-2	[−1, 64, 112, 112]	128	Conv2d-131
ReLU-3	[−1, 64, 112, 112]	0	BatchNorm2d-132
MaxPool2d-4	[−1, 64, 56, 56]	0	ReLU-133
Conv2d-5	[−1, 64, 56, 56]	4,096	Conv2d-134
BatchNorm2d-6	[−1, 64, 56, 56]	128	BatchNorm2d-135
ReLU-7	[−1, 64, 56, 56]	0	ReLU-136
Conv2d-8	[−1, 64, 56, 56]	36,864	Conv2d-137
BatchNorm2d-9	[−1, 64, 56, 56]	128	BatchNorm2d-138
ReLU-10	[−1, 64, 56, 56]	0	ReLU-139
Conv2d-11	[−1, 256, 56, 56]	16,384	Bottleneck-140
BatchNorm2d-12	[−1, 256, 56, 56]	512	Conv2d-141
Conv2d-13	[−1, 256, 56, 56]	16,384	BatchNorm2d-142
BatchNorm2d-14	[−1, 256, 56, 56]	512	ReLU-143
ReLU-15	[−1, 256, 56, 56]	0	Conv2d-144
Bottleneck-16	[−1, 256, 56, 56]	0	BatchNorm2d-145
Conv2d-17	[−1, 64, 56, 56]	16,384	ReLU-146
BatchNorm2d-18	[−1, 64, 56, 56]	128	Conv2d-147
ReLU-19	[−1, 64, 56, 56]	0	BatchNorm2d-148
Conv2d-20	[−1, 64, 56, 56]	36,864	Conv2d-149
BatchNorm2d-21	[−1, 64, 56, 56]	128	BatchNorm2d-150
ReLU-22	[−1, 64, 56, 56]	0	ReLU-151
Conv2d-23	[−1, 256, 56, 56]	16,384	Bottleneck-152
BatchNorm2d-24	[−1, 256, 56, 56]	512	Conv2d-153
ReLU-25	[−1, 256, 56, 56]	0	BatchNorm2d-154
Bottleneck-26	[−1, 256, 56, 56]	0	ReLU-155
Conv2d-27	[−1, 64, 56, 56]	16,384	Conv2d-156
BatchNorm2d-28	[−1, 64, 56, 56]	128	BatchNorm2d-157
ReLU-29	[−1, 64, 56, 56]	0	ReLU-158
Conv2d-30	[−1, 64, 56, 56]	36,864	Conv2d-159
BatchNorm2d-31	[−1, 64, 56, 56]	128	BatchNorm2d-160
ReLU-32	[−1, 64, 56, 56]	0	ReLU-161
Conv2d-33	[−1, 256, 56, 56]	16,384	Bottleneck-162
BatchNorm2d-34	[−1, 256, 56, 56]	512	Conv2d-163
ReLU-35	[−1, 256, 56, 56]	0	BatchNorm2d-164
Bottleneck-36	[−1, 256, 56, 56]	0	ReLU-165
Conv2d-37	[−1, 128, 56, 56]	32,768	Conv2d-166
BatchNorm2d-38	[−1, 128, 56, 56]	256	BatchNorm2d-167
ReLU-39	[−1, 128, 56, 56]	0	ReLU-168
Conv2d-40	[−1, 128, 28, 28]	147,456	Conv2d-169
BatchNorm2d-41	[−1, 128, 28, 28]	256	BatchNorm2d-170
ReLU-42	[−1, 128, 28, 28]	0	ReLU-171
Conv2d-43	[−1, 512, 28, 28]	65,536	Bottleneck-172
BatchNorm2d-44	[−1, 512, 28, 28]	1,024	AvgPool2d-173
Conv2d-45	[−1, 512, 28, 28]	131,072	Linear-174
BatchNorm2d-46	[−1, 512, 28, 28]	1,024	Total params: 25,557,032
ReLU-47	[−1, 512, 28, 28]	0	Trainable params: 25,557,032
Bottleneck-48	[−1, 512, 28, 28]	0	Non-trainable params: 0
Conv2d-49	[−1, 128, 28, 28]	65,536	Input size (MB): 0.57
BatchNorm2d-50	[−1, 128, 28, 28]	256	Forward/backward pass size (MB): 286.56
ReLU-51	[−1, 128, 28, 28]	0	Params size (MB): 97.49
Conv2d-52	[−1, 128, 28, 28]	147,456	Estimated Total Size (MB): 384.62
BatchNorm2d-53	[−1, 128, 28, 28]	256	...

# Deeper is better





Finding the optimal neural network architecture remains an **active area of research**.

# Pre-trained models

- Training a model on natural images, from scratch, takes **days or weeks**.
- Many models trained on ImageNet are publicly available for download. These models can be used as **feature extractors** or for smart **initialization**.

## Transfer learning

- Take a pre-trained network, remove the last layer(s) and then treat the rest of the the network as a **fixed** feature extractor.
- Train a model from these features on a new task.
- Often better than handcrafted feature extraction for natural images, or better than training from data of the new task only.

## Fine tuning

- Same as for transfer learning, but also **fine-tune** the weights of the pre-trained network by continuing backpropagation.
- All or only some of the layers can be tuned.

In the case of models pre-trained on ImageNet, this often works even when input images for the new task are not photographs of objects or animals, such as biomedical images, satellite images or paintings.

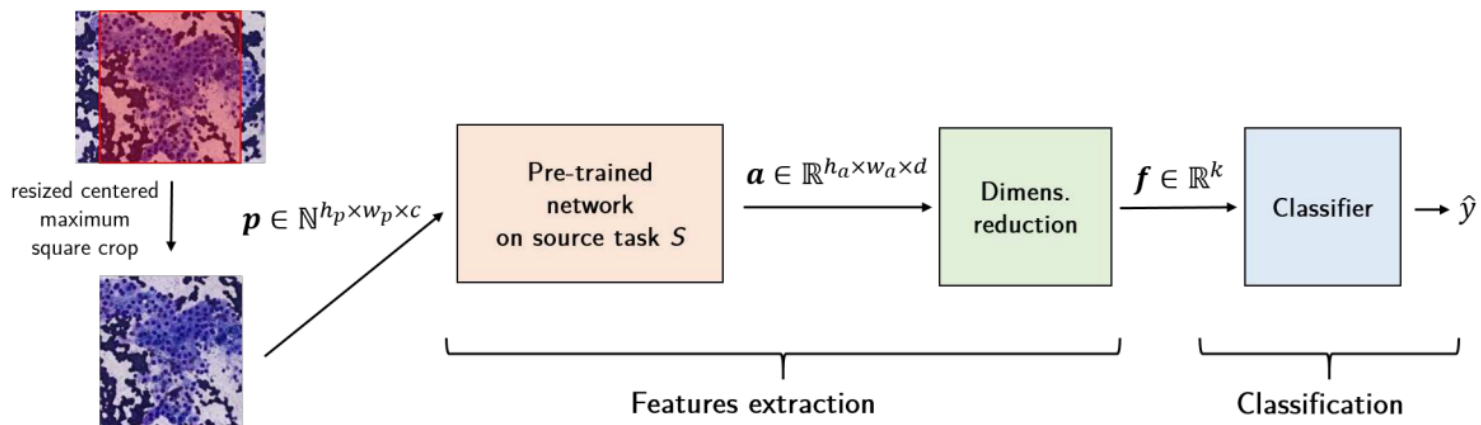


Figure 2. Feature extraction from pre-trained convolutional neural networks

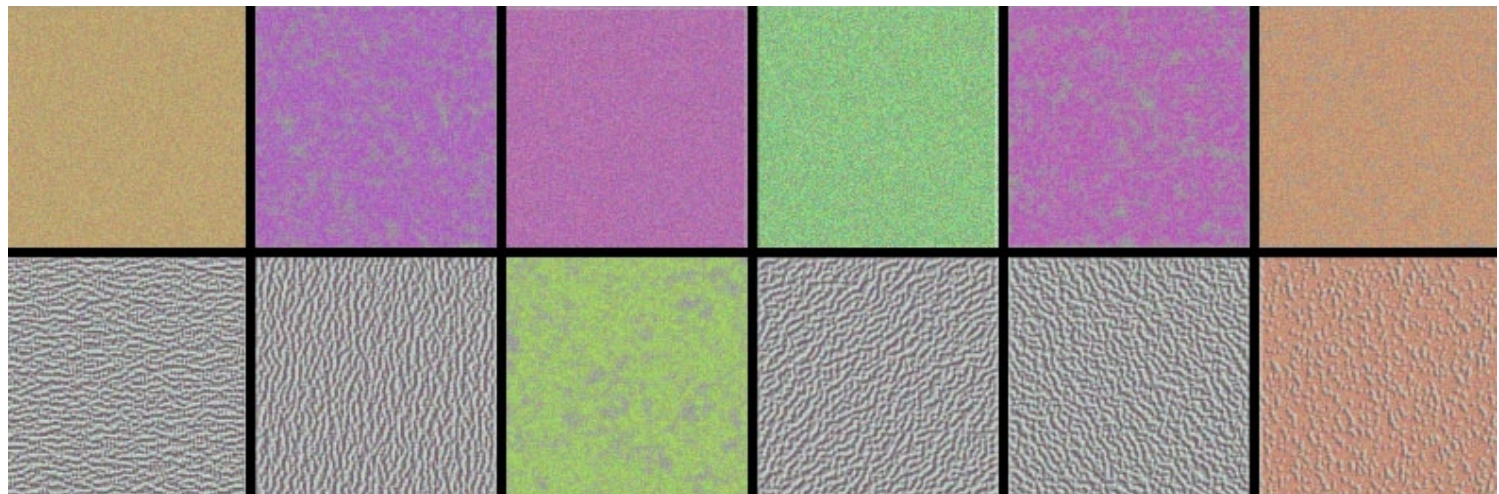
# **What is really happening?**

# Maximum response samples

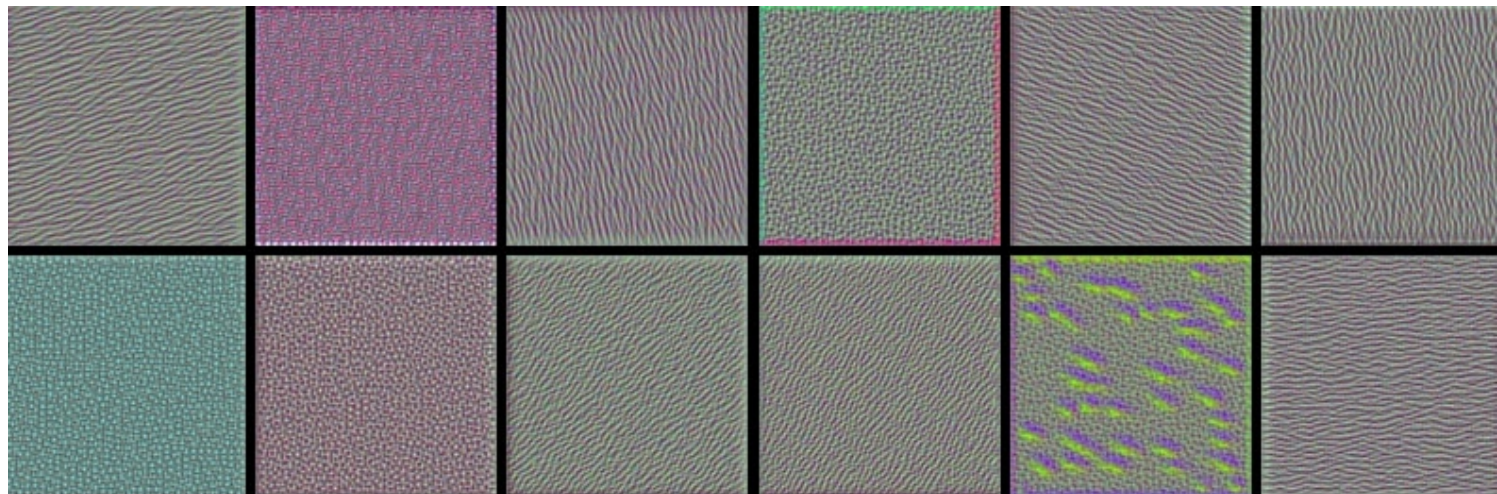
Convolutional networks can be inspected by looking for input images  $\mathbf{x}$  that maximize the activation  $\mathbf{h}_{\ell,d}(\mathbf{x})$  of a chosen convolutional kernel  $\mathbf{u}$  at layer  $\ell$  and index  $d$  in the layer filter bank.

Such images can be found by gradient ascent on the input space:

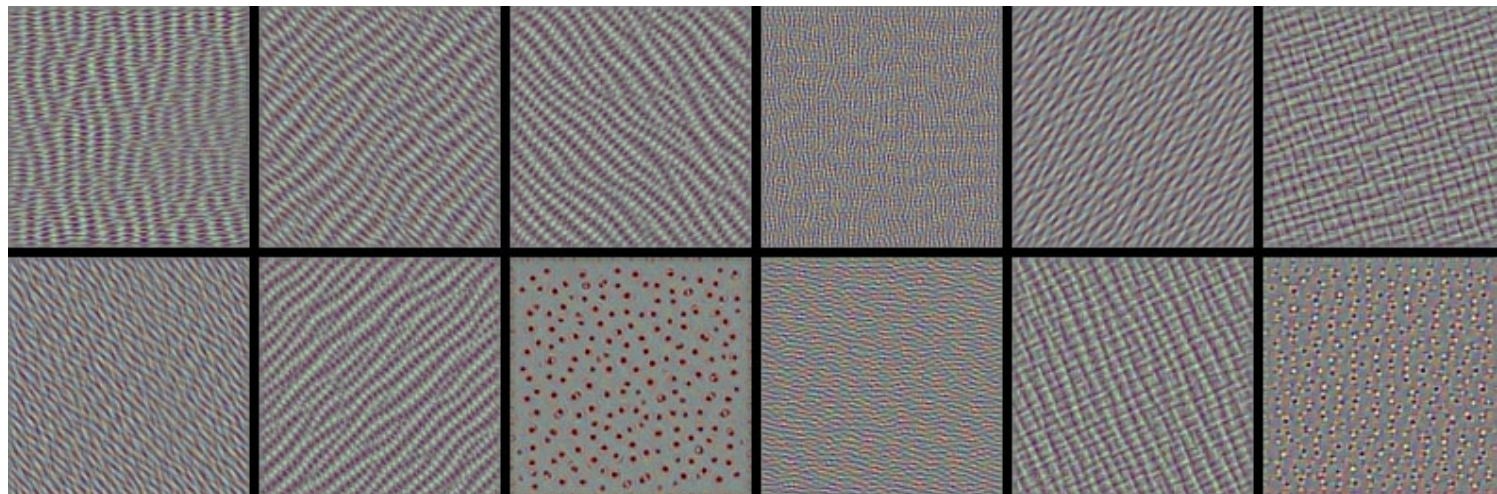
$$\begin{aligned}\mathcal{L}_{\ell,d}(\mathbf{x}) &= \|\mathbf{h}_{\ell,d}(\mathbf{x})\|_2 \\ \mathbf{x}_0 &\sim U[0, 1]^{C \times H \times W} \\ \mathbf{x}_{t+1} &= \mathbf{x}_t + \gamma \nabla_{\mathbf{x}} \mathcal{L}_{\ell,d}(\mathbf{x}_t)\end{aligned}$$



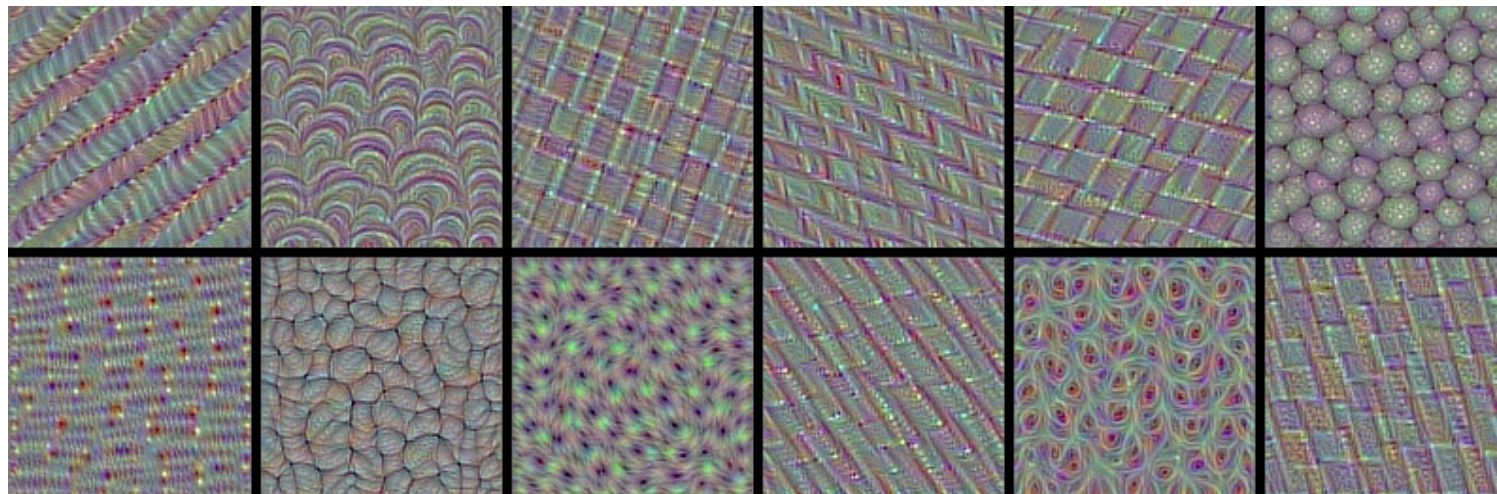
VGG-16, convolutional layer 1-1, a few of the 64 filters



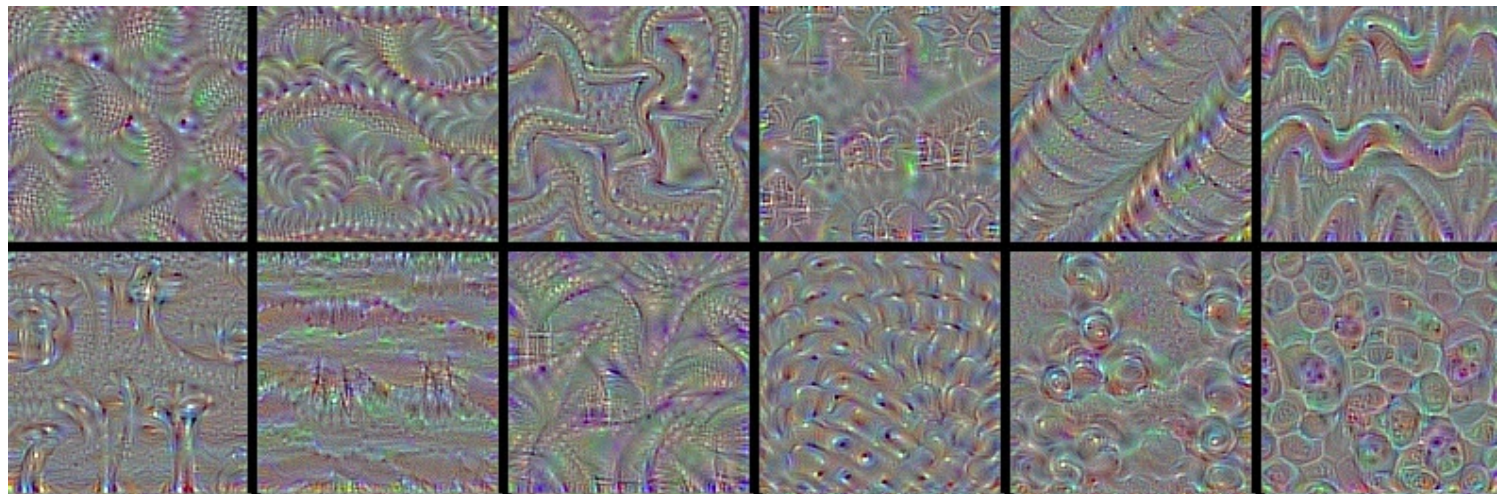
VGG-16, convolutional layer 2-1, a few of the 128 filters



VGG-16, convolutional layer 3-1, a few of the 256 filters



VGG-16, convolutional layer 4-1, a few of the 512 filters

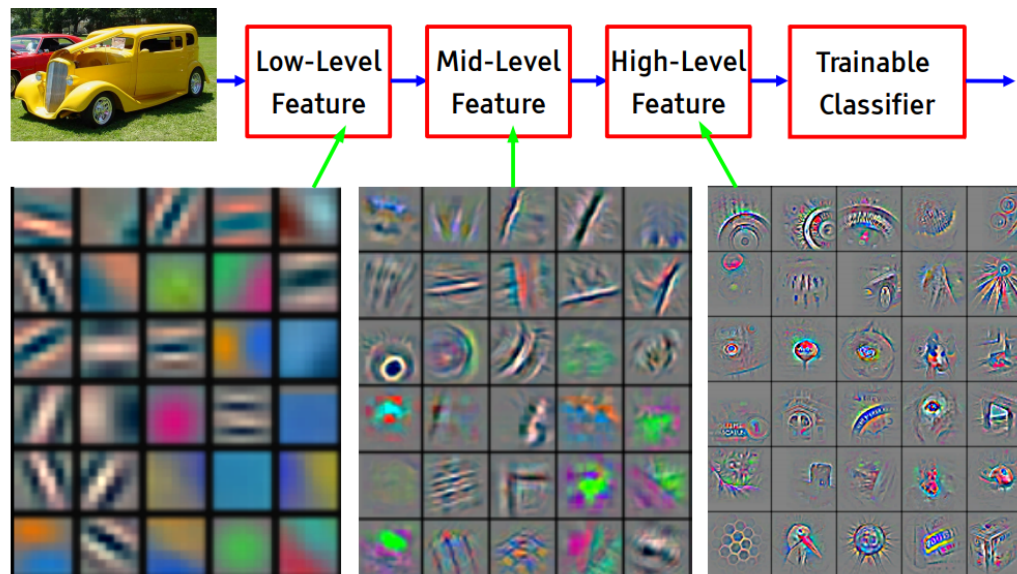


VGG-16, convolutional layer 5-1, a few of the 512 filters

Some observations:

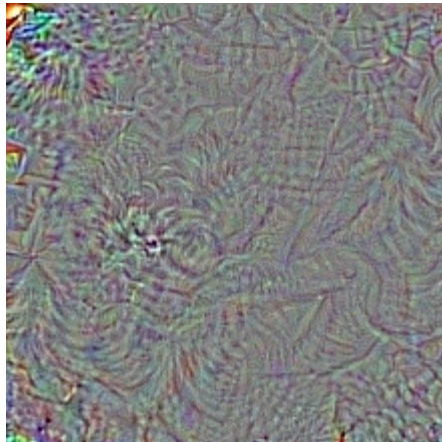
- The first layers appear to encode direction and color.
- The direction and color filters get combined into grid and spot textures.
- These textures gradually get combined into increasingly complex patterns.

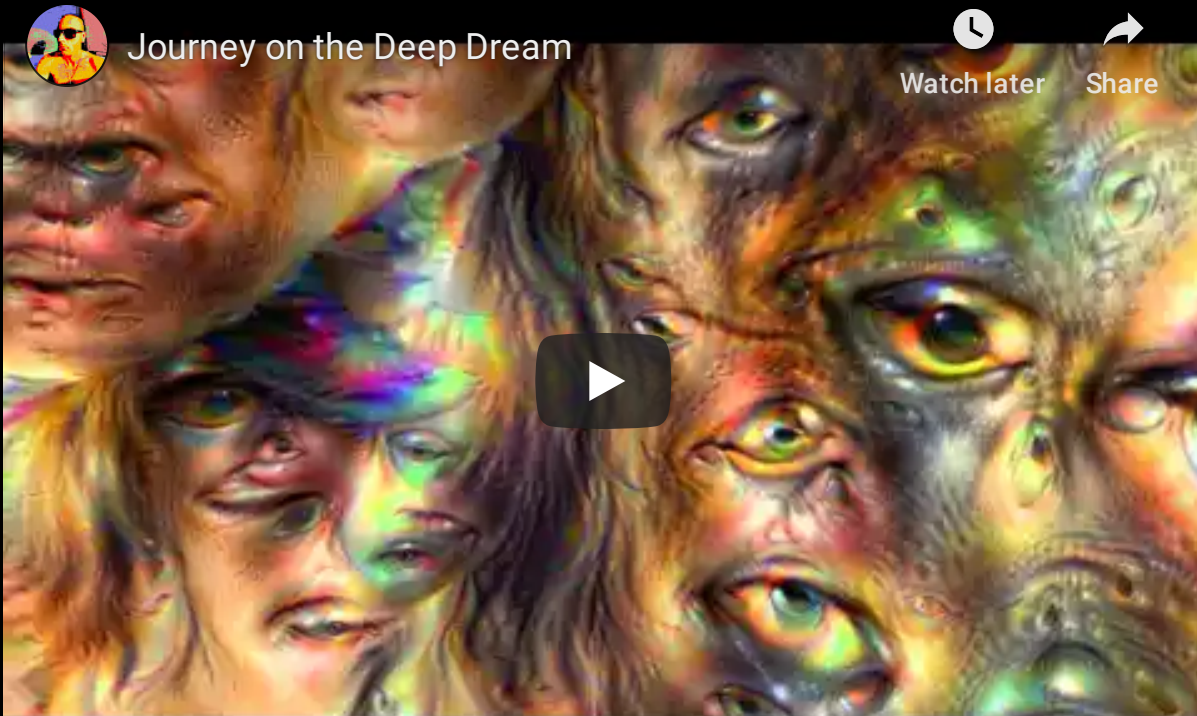
In other words, the network appears to learn a hierarchical composition of patterns.



Feature visualization of convolutional net trained on ImageNet from [Zeiler & Fergus 2013]

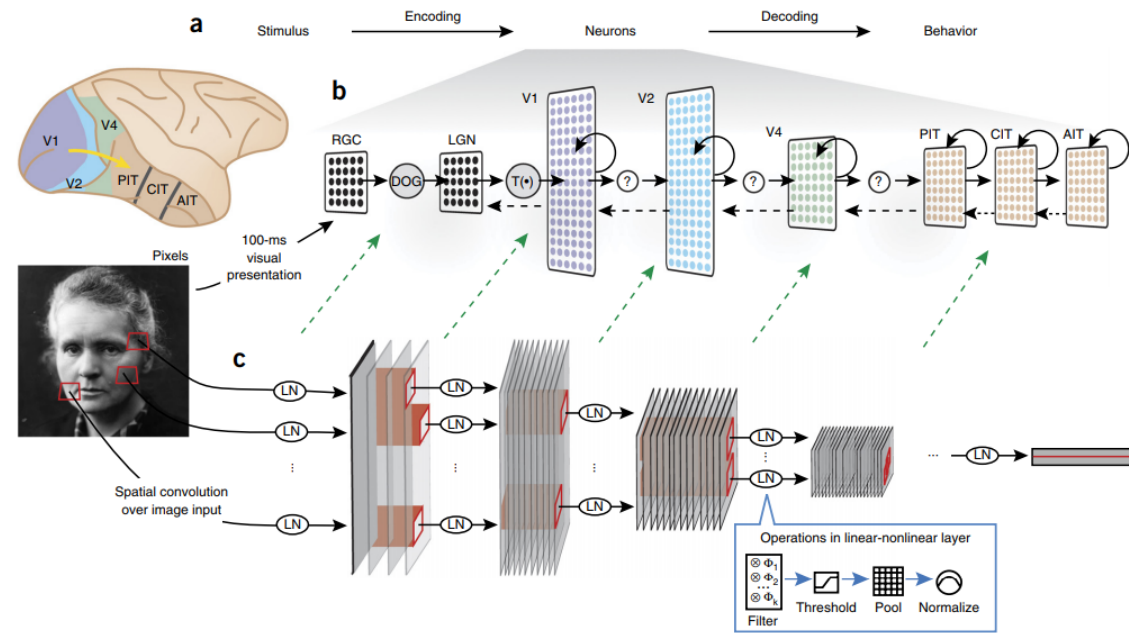
What if we build images that maximize the activation of a chosen class output?  
The left image is predicted **with 99.9% confidence** as a magpie!





**Deep Dream.** Start from an image  $\mathbf{x}_t$ , offset by a random jitter, enhance some layer activation at multiple scales, zoom in, repeat on the produced image  $\mathbf{x}_{t+1}$ .

# Biological plausibility



*"Deep hierarchical neural networks are beginning to transform neuroscientists' ability to produce quantitatively accurate computational models of the sensory systems, especially in higher cortical areas where neural response properties had previously been enigmatic."*

The end.

# References

- Francois Fleuret, Deep Learning Course, [4.4. Convolutions](#), EPFL, 2018.
- Yannis Avrithis, Deep Learning for Vision, [Lecture 1: Introduction](#), University of Rennes 1, 2018.
- Yannis Avrithis, Deep Learning for Vision, [Lecture 7: Convolution and network architectures](#), University of Rennes 1, 2018.
- Olivier Grisel and Charles Ollion, Deep Learning, [Lecture 4: Convolutional Neural Networks for Image Classification](#), Université Paris-Saclay, 2018.